Chapter 23

Saccade Slowing After Lesions of Omnipause Neurons Explained By Two Hypothetical Membrane Properties of Premotor Burst Neurons

Kenichiro Miura and Lance M. Optican

1. INTRODUCTION

Chemical lesions of the brain stem region containing omnipause neurons (OPNs) slow saccades without consistent changes in reaction time. Previous models with simple elements have not been able to explain these results. This study proposes a hypothetical mechanism for saccade slowing, based on a more detailed model of medium-lead burst neurons (MLBNs) than has been used in previous models. The MLBN element used in this study has two biophysical properties, a post-inhibitory rebound depolarization and a threshold for firing. In our model, for a normal saccade, the offset of the OPN induces a post-inhibitory rebound depolarization while MLBNs are receiving an excitatory input (drive) from long lead burst neurons (LLBNs). Thus, the rebound depolarization caused by the OPN offset is added to this drive input. After an OPN lesion, the additional drive, which would occur in response to OPN offset under normal conditions, would be absent, resulting in saccades that are slower than normal. The role of the threshold in the MLBN model is to prevent the eyes from drifting before the saccade starts. Thus, the threshold must be higher than the prelude input from LLBNs. This maintains the reaction time of saccades even after an OPN lesion. A computer simulation of a saccadic model that incorporates an MLBN with these two membrane properties produces behavioral changes in saccades after simulated OPN lesion that are consistent with experimental findings. The new model also suggests potential experiments to test the MLBN properties proposed here.

Medium lead burst neurons (MLBNs; also referred to as short lead burst neurons) are the premotor neurons for saccades, the rapid eye movements used for re-fixation. MLBNs consist of excitatory and inhibitory burst neurons (EBNs and IBNs) distributed in the midbrain, pons and medulla [1-3]. For example, EBNs making horizontal saccades are in the pontine reticular formation (RF), projecting to ipsilateral abducens nucleus (ABD), and IBNs for horizontal saccades are in the medullary RF, projecting to contralateral ABD [4-8]. The activities of these MLBNs are closely related to the properties of saccades [6-10]. For example, their bursts start just before the beginning of ipsilateral saccades; the duration of the burst is closely related to saccadic duration; and the total number of spikes in the burst activity during ipsilateral saccades is proportional to the amplitude of the saccades. Thus, it is commonly assumed that the MLBNs provide the drive command for a saccade.

The system generating saccades also includes another class of brain stem neurons, referred to as *omnipause* neurons (OPNs). In awake animals, OPNs have tonic activity that ceases during saccades in any directions [9, 11, 12]. In primates, OPNs are located in

the pontine nucleus raphe interpositus, RIP [13]. Single unit recordings from monkeys and cats have demonstrated that the pause of OPNs, caused by a hyperpolarization of their membrane potential, starts just before MLBNs begin firing [9, 14]. The duration of the pause, or hyperpolarized state, of OPNs is closely correlated with saccadic duration [9, 14]. Anatomical findings demonstrated that OPNs project most densely to regions containing EBNs and IBNs [15, 16]. Stimulation in the OPN region during saccades stops movements of the eyes immediately [17]. Because of these observations, it is commonly assumed that OPNs inhibit MLBNs, acting as an inhibitory gate for the driving system of the saccades.

Since Robinson's seminal work [18], many similar models for the control of saccades have been proposed. In classical models [10, 18-20], the saccadic system has been commonly described as a negative feedback control circuit. Recent studies have focused more on neural processing (neural networks) for motor control of saccades, based on discoveries of details of saccade-related neural activity in the brain stem (pons and superior colliculus: SC) and in the cerebellum [21-26]. The functional roles of the cerebellum and/or the SC in saccades has been intensively studied [22, 24-27]. Despite this progress, MLBNs in recent models have still been assumed to have only very simple properties, such as a single time constant [24], a firing rate saturation [22, 25], both [23], or a simple delay [21]. Thus, in the classical scheme only a simple role could be assigned to the MLBNs.

Kaneko [28] demonstrated that the peak velocity of saccades was decreased when the RIP, which contains OPNs, is damaged by injecting ibotenic acid. Recently the same phenomenon was reproduced by muscimol injections into the same brain stem region. RIP lesions significantly changed the dynamic features of saccades; there was a decrease in the peak velocity and an increase in saccadic duration [29]. However, other characteristics were normal, including saccadic accuracy and reaction time. The normal accuracy suggests that saccades are made under feedback control. This is consistent with classical findings [20, 30] and is the basis of the Robinson model structure (1975), and thus all subsequent saccadic models can explain this property. An extended saccadic duration is a natural consequence of a feedback controller with a slower eye velocity (perhaps due to a smaller drive signal), and thus is also explained by older models.

However, no model has explained why RIP lesions cause saccade slowing without a change in reaction time. A model for saccade generation proposed by Scudder [21] exhibits the decrease in peak velocity when OPNs are inactivated to simulate the effect of RIP lesion, but the decrease in peak velocity must be accompanied by a shortening of reaction times of saccades [31]. If the reaction time stayed the same, there would be no decrease in saccadic velocity (see Discussion). In contrast, the lesion studies strongly suggest that the decrease in peak velocity is not correlated with a reduction of saccadic reaction times [29]. The reaction time was significantly increased after an OPN lesion in 3 of 14 cases, was decreased in one case, and in 10 of 14 cases there was no significant change in saccadic reaction time. Thus, the prediction from Scudder's model does not fit the data. Therefore, another mechanism for slowing down saccades, which does not depend upon changes in saccadic reaction time, is needed.

Ramat et al. [32] have pointed out a possible dependence of saccadic oscillations on a hypothesized membrane property of MLBNs: post-inhibitory rebound depolarization (leading to post-inhibitory rebound firing), suggesting a possible contribution of OPN

offset and the post-inhibitory rebound depolarization of MLBNs to saccadic generation. In this study, we adopt the assumption that the post-inhibitory rebound depolarization caused by OPN offset provides an additional drive signal for saccades. It is possible that this assumed rebound depolarization could also explain the phenomena found by Kaneko's group [28, 29], i.e., saccade slowing after RIP lesion. Computer simulations of a model of the saccadic system that incorporates the MLBN model from Ramat et al. do generate slow saccades after a simulated OPN lesion. However, these slow saccades show a pronounced early drift. Therefore, we add a second assumption to the model, that the MLBN also has a threshold, below which inputs can not elicit any output. These two assumptions are sufficient to demonstrate saccade slowing without a change in reaction time. We will also discuss potential experiments to test the hypothesis proposed in this study. Brief, preliminary reports have appeared previously [33, 34].

2. THE NEW MODEL

First, we will give a brief explanation of the hypothetical mechanism that may underlie the saccade slowing after an RIP lesion. Then, we will describe the implementation of this model as it was used in our simulations. Here, we propose a generic model of saccade generation which has a new MLBN element. The purpose of the implementation made here is to explain a possible, novel function of inhibitory input from OPNs to MLBNs and a hypothetical mechanism of saccade slowing after an OPN lesion. (NB: this model is not designed to reflect the biophysical mechanisms that create these properties.)

2.1 POST-INHIBITORY REBOUND

Our hypothesis for saccade slowing after an RIP lesion relies on a hypothetical membrane property of MLBNs: post-inhibitory rebound depolarization. If MLBNs have this property, OPN offset will induce rebound depolarization of MLBNs, as previously suggested [32]. It is likely for a normal saccade that OPN offset occurs while MLBNs are receiving the burst input from long lead burst neurons (LLBNs) in their upstream regions. For example, it has been suggested that MLBNs may receive a mono-, di- or poly-synaptic input from the superior colliculus [35, 36], in which saccade-related neurons begin to burst approximately 20 ms before saccade onset [37]. Yoshida et al. [14] have demonstrated by intracellular recordings that the steep hyperpolarization of membrane potential of OPNs begins about 16 ms before saccade onset. Thus, the rebound depolarization caused by the OPN offset on MLBNs will be added to the excitatory drive input. The effect of the post-inhibitory rebound depolarization will be to make the saccades faster than they would be with the input from the LLBNs alone. This idea suggests a hypothetical mechanism underlying the effect of RIP lesions on saccadic speed. It is assumed that OPNs are damaged or inactivated after an RIP lesion. Then, the additional drive, which would occur in response to OPN offset under normal conditions, would be absent after RIP lesions. Therefore, saccades would be slower. It is important to note that this hypothetical mechanism is independent of any changes in reaction time,

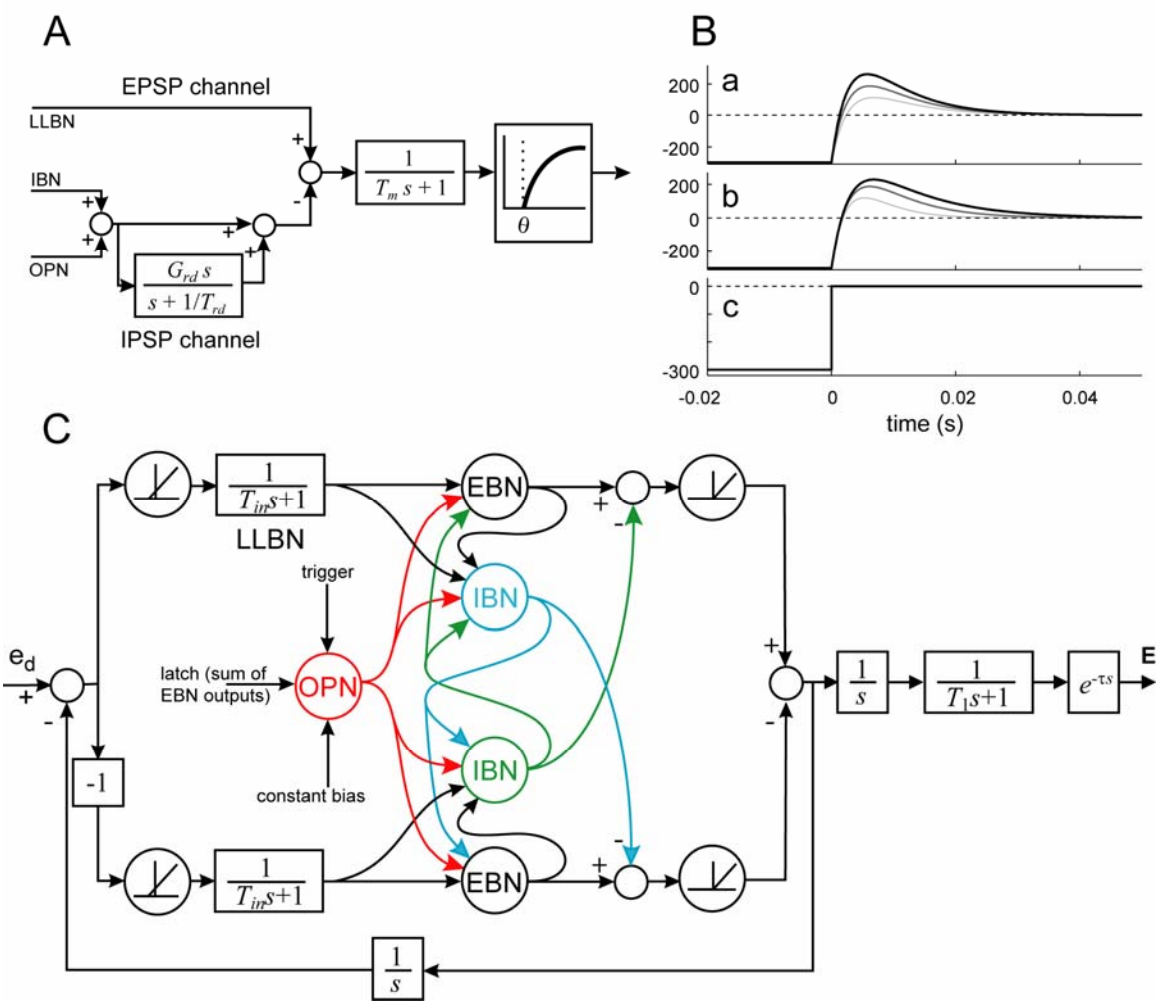

Figure 1. A: A block diagram of the lumped model of a medium-lead burst neuron. The model has two channels for its membrane state dynamics: EPSP and IPSP channels that mediate the change in membrane state caused by an excitatory drive input from LLBNs and by inhibitory inputs from OPN and contralateral IBN, respectively. The dynamic properties of model MLBNs are lumped into two transfer functions: one low-pass property (time constant of Tm, which was set to 3 ms in the simulations shown in the next section) that affects both EPSP and IPSP channels, and the other specifically for the dynamics of IPSPs, i.e., a high pass filter in a side path of the IPSP channel that mediates post-inhibitory rebound depolarization. The output function that transforms membrane state to firing rate has a saturation property and a threshold, θ. See text for further details. B: Temporal profiles of membrane state (a and b) after the offset of inhibitory signal (c) of the MLBN model in A. B-a: Temporal profiles of membrane state for different Grd values of 0.5 (light gray line), 1.0 (dark gray line) or 1.5 (black line) with constant Trd (=7ms). B-b: Temporal profiles of membrane state for different Trd values of 4 ms (light gray line), 7 ms (dark gray line) or 10 ms (black line) with constant G_{rd} (=1). B-c: Time course of OPN. C: The complete model of the saccadic system used for simulations in this paper. The details of MLBNs are shown in A. T_{in}, T_1 and □ were fixed at 7, 5 and 9 ms, respectively. To avoid clutter in the figure, delay and gain elements on connections among MLBNs, and details of the OPN unit, are omitted. Colored arrows are inhibitory signals. See text for more details.

because no specific changes in reaction time with saccade slowing were observed by Kaneko and colleagues.

2.2 MLBN ELEMENT

Here, we model the effects on saccade speed of pre-saccadic inhibition of MLBNs by OPNs. We implemented MLBNs with a lumped model to explain this. We did not intend to model detailed biophysical features (such as morphology of the neuron, properties of ion channels and so on), which are not known for MLBNs. Here, we prefer a lumped implementation describing functions which incorporate many uncertain details to keep the proposed model simple.

Our model of MLBNs has a membrane property of post-inhibitory rebound depolarization. The schematic diagram of the model of MLBNs is illustrated in Fig. 1A, as a block diagram (where s is the Laplace transform variable; the saccade drive, which is essentially a velocity signal, is in deg/s.). In our implementation, we explicitly dissociated two types of inputs, i.e., excitatory (EPSP channel) and inhibitory (IPSP channel) to clarify their functions on the membrane state of MLBNs during saccades. The EPSP channel mediates the change in membrane state caused by excitatory inputs from upstream LLBNs. The IPSP channel mediates the change in membrane state caused by inhibitory inputs, which in our model come from the OPN and the contralateral IBN unit (for the entire circuit, see Fig. 1C.) The membrane state dynamics of the model neuron is lumped into two computational elements. One is an element that affects the membrane state dynamics caused both by excitatory and inhibitory inputs, i.e., a low pass filter with a time constant (T_m) that was set to 3 ms in the simulations shown in this paper. (The value of T_m is not important for the property of saccade slowing caused by OPN lesions. A preliminary simulation study showed that changing T_m from one to five ms did not change general properties of the saccade slowing in our model.)

Generally, a negative feedback system with a large time constant (such as the one in Fig. 1C) causes oscillatory behaviors. However, the saccadic system does not usually oscillate. We have assumed that the loop already includes a relatively long time constant (7 ms, see below) as a property of the input to MLBNs from LLBNs. Therefore, the MLBN, which is also inside the loop, has to have a small time constant (such as the values we used here) to satisfy this behavioral constraint.

The other element models the effect of inhibitory inputs on the membrane state. This is implemented as a high pass filter on the IPSP channel. In the present implementation, the post-inhibitory rebound depolarization is controlled by two parameters: G_{rd} and T_{rd}. G_{rd} determines the magnitude of rebound depolarization (Fig. 1B-a). T_{rd} denotes the time constant of the decay of rebound depolarization (Fig. 1B-b). Because of the common low pass property ($1/(T_m s+1)$), T_{rd} also modifies the magnitude of resultant rebound firing. We used T_{rd}'s of 1-10 ms in the following simulations. (A T_{rd} of more than 10 ms also exhibits saccade slowing after OPN lesion. However, a relatively smaller time constant is more reasonable as a post-inhibitory effect of inhibitory signals on MLBNs, because too large a T_{rd} causes post-inhibitory rebound whose duration is longer than that of typical saccades. See also Discussion). In the previous model for saccadic oscillations [32] and in our preliminary studies [33, 34], the high pass filter was assumed to be on the pathway after both EPSP and IPSP channels are merged, because a single channel was assumed in these models. We prefer the present implementation in which T_{rd} and G_{rd} have simpler roles in membrane state dynamics in the MLBN model than the previous ones. That is, this change affects only the dynamics of membrane state that are mediated by IPSPs, in particular that of post-inhibitory rebound depolarization

during saccades. This is not a fundamentally different model in our functional implementation, but the change simplifies the simulations because it decouples the parameters of the rebound mechanism from the LLBN outputs. (Note that combining the IPSP and EPSP channels before the high pass filter would not change saccadic latency or peak velocity, because rebound from excitation only inhibits the cell, which is what resumption of OPNs is trying to do, anyway.)

To resolve the effect of OPN lesions on the reaction time of saccades, we have also introduced a threshold for firing. It has been suggested that the sources of input to MLBNs include LLBNs in the superior colliculus [35], pons [38] and fastigial nuclei [39]. LLBNs in these areas commonly show activity lasting from long before the saccades in their "on direction" (referred to as build-up, prelude or sustained activity), followed by an intense burst component with a relatively long lead time [9, 37, 40]. The input to the MLBNs in our simulations has the characteristics seen in these neurons, in particular, the prelude component. Prior saccade models depend on the OPNs to inhibit the MLBNs before the saccade starts, thus preventing a response to prelude inputs, and preventing the eyes from drifting slowly before saccades. These previous models all predict a shorter reaction time after OPN lesion in the presence of the prelude activity, because the OPNs alone block the prelude activity. Nonetheless, the experimental findings suggest that there must be another mechanism capable of blocking the prelude activity. We hypothesize here that this blocking may be achieved by a membrane property of MLBNs: a threshold for firing. The threshold (denoted as θ) is incorporated into the output function of MLBNs that transforms membrane state to firing rate. The output function of MLBNs is defined as:

$$f_b(u) = \begin{cases} a(1 - e^{-(u-\theta)/b}) & (u > \theta) \\ 0 & (otherwise) \end{cases} \qquad (1),$$

where a and b are constants set to 1000 and 300 (deg/s), respectively; u is the input variable; θ was adjusted so that the model showed the expected behaviors (see below).

2.3 THE ENTIRE SYSTEM

In this study, we simulated saccades with a lumped system, but with relatively detailed premotor structures (Fig.1C). The connections among MLBNs are the same as those of the saccadic oscillation model proposed by Ramat et al. [32]. They introduced detailed features of brain stem circuitry to distribute MLBNs into four populations: EBNs and IBNs in left and right brain stem. EBNs project to ipsilateral IBNs with a delay of 1 ms, which then project to contralateral EBNs and IBNs, again with delay of 1 ms. (These delay elements are not shown in Fig. 1C to reduce clutter.) Here, the same MLBN model is used for both EBNs and IBNs.

The excitatory input to MLBNs in the present simulation system has two temporal phases: *prelude* and *drive*. For ipsilateral saccades, in the prelude phase, the input was simply defined as a constant (it was set to 30 deg/s in simulations). In the drive phase, the input is related to motor error, representing the burst component in the input from LLBNs. (This configuration is based on the most likely hypothesis that SC, the cerebellum or the both of them is involved in feedback controls. As described above, these structures may project to the saccadic premotor structures directly or indirectly.) First, the transformed motor error $\phi_{hr}(C_1\hat{e}_m + C_0)$ is calculated, where C_1 and C_0 are

constants that were adjusted so that the model showed expected saccadic behavior, $\hat{e}_m$ denotes estimated motor error that is defined by the desired eye displacement (e_d) minus the estimated eye displacement (temporal integration of the input to the final common path, see below for definition), ϕ_{hr} denotes a half-wave rectification function (i.e., passes only positive signals). Then the transformed motor error is fed to MLBNs through a low pass filter whose time constant (T_{in}) was set to 7 ms to simulate the somewhat sluggish development of the burst activity of LLBNs [8]. For contralateral saccades, the input was set to 0 in the prelude phase. In the drive phase, the input is calculated in the same way as that for ipsilateral saccades, but by replacing $\hat{e}_m$ with $-\hat{e}_m$. C_0 was set to $\dot{\theta}$- 3, just below $\dot{\theta}$ so that small motor errors would still elicit saccades and that larger saccades would not end while there was still a large residual motor error. The small dead zone for very small motor error helps to prevent system oscillations due to the negative feedback system property, without causing major changes in saccadic amplitude. Both EBNs and IBNs receive the same input.

The OPN unit projects to all MLBNs. The OPN unit is defined in a quite similar manner to that of classical models [10]. The detail of the OPN unit is omitted from Fig. 1C for the simplicity. The state of the OPN unit is defined by the sum of a constant bias, OPN_{in} (= 600 deg/s, this value was selected so that the OPN unit could inhibit the MLBNs), a brief inhibitory trigger (30 ms inhibitory pulse starting at OPN_{off} (ms) after the onset of the burst component in the input from LLBNs to MLBNs, with the same magnitude as the constant bias) and an inhibitory latch signal. The magnitude of the latch signal is defined as the sum of outputs of left and right EBNs weighted by 20. The state was rectified with the function ϕ_{hr} and then this signal was fed to the IPSP channels on MLBNs through a low pass filter with a time constant of T_{opn} (which was set to 3 ms in the following simulation). Note that T_{opn} does not correspond to the time constant of the population activity of OPNs, but simulates the time constant of the effect of OPN activity on MLBN membrane state. T_{opn} affects the post-inhibitory rebound depolarization caused by OPN offset as T_{rd}. Larger or smaller T_{opn} exhibits slower or faster decay of post-inhibitory rebound depolarization. Although the exact value for this time constant is unknown, we prefer to use a small value here because of the same reason as that for the choice of the range of T_{rd}. Because of the similarity of function between T_{opn} and T_{rd} on the post-inhibitory rebound depolarization, the effect of modifying T_{opn} on the temporal property of the rebound depolarization can be cancelled by changing T_{rd}. We used this strategy here. In the proposed model, the relationship among G_{rd}, T_{rd} and T_{opn} is more critical. In particular, when T_{rd} is smaller than T_{opn}, choosing G_{rd} so that it becomes larger than (T_{opn} / T_{rd})–1 is important, otherwise the post-inhibitory rebound (the overshoot property shown in Fig. 1 B) does not occur.

The downstream pathway from MLBNs (including motoneurons, the neural integrator, ocular muscles, and globe) was represented by an integrator, a low pass filter with an uncompensated time constant (5 ms), and a delay element (9 ms, representing the latency of saccades from the onset of MLBN activity, see Keller [9]). The signal sent to this structure is defined in the same manner as that by Lefèvre et al. [24] and is given by $\phi_{hr}\left(EBN_i(t) - IBN_c(t)\right) - \phi_{hr}\left(EBN_c(t) - IBN_i(t)\right)$, EBN_i, EBN_c, IBN_i and IBN_c denote outputs of EBN ipsilateral, EBN contralateral, IBN ipsilateral and IBN contralateral relative to the direction of the saccade. The same signal is fed back and integrated to estimate the

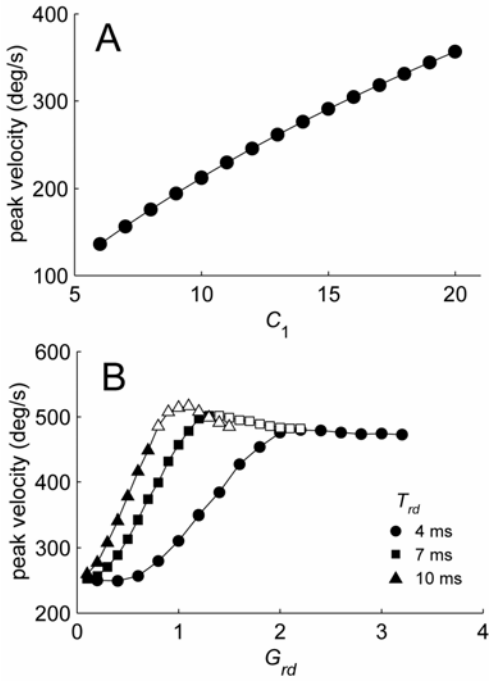

Figure 2. Model properties. **A**: Peak velocity of saccades caused by LLBN output alone as a function of C_1. OPN_{in} was set to 0 to generate these saccades. θ was adjusted so that the latency of saccades was within 20±1 ms from the onset of the drive phase of the LLBN output. The onset of eye movements was determined as the time when the eye velocity first exceeded 10 deg/s. **B**: Peak velocity of saccades when OPN is normal, as a function of G_{rd} for three T_{rd}'s (circles for 4 ms, squares for 7 ms and triangles for 10 ms). Open symbols indicate peak velocity of saccades with post-saccadic oscillations (dynamic overshoots) of more than 50 deg/s in amplitude. OPN_{off} was adjusted so that the latency of saccades was again within 20±1 ms after the onset of the drive phase of the LLBN output.

current displacement that is, in turn, used to calculate the estimate of motor error (see above). Note that the units of activities of OPN and the input from LLBNs are the saccade drive, which is essentially a velocity signal, with units of deg/s. The time course of each element in the entire system is described in the next section (see Fig. 3 for sample profiles).

3. RESULTS

The purpose of the present simulation study is twofold. One is to see if the model can produce behaviors that are consistent with experimental findings from putative OPN inactivation studies. The other is to find inherent properties of the model that are testable by future experimental studies. The simulations were performed on a personal computer with MATLAB and SIMULINK (The MathWorks, Natick, MA).

3.1 MODEL PROPERTIES

The properties of saccades that we are primarily concerned with in the present study were obtained by adjusting several parameters. C_1 regulates the speed of saccades driven by the excitatory input from the LLBN alone (Fig. 2A). Thus, this parameter determines the peak velocity of saccades when the OPN is inactivated. When the OPN is active, i.e., in normal condition, the other parameters also regulate peak velocity of saccades. The peak velocity of saccades in the normal case increased to some extent as G_{rd} was increased and covered a physiologically realistic range of saccadic peak velocity before it saturated (Fig. 2B). The saturations seen for larger G_{rd} are in large part due to the output of MLBNs contralateral to the ongoing saccades. This saturation has no effect on the properties studied here, and it may simply be an artifact of our specific implementation of the model (see below for more details). As shown in Fig. 2B, T_{rd} also

	T_{rd} (ms)	G_{rd}	OPN_{off} (ms)	*PV* (deg/s)	*Amp* (deg)
1	1	8.0	6	436.5	9.6
2	2	4.0	6	454.6	9.8
3	3	2.4	5	448.4	9.8
4	4	1.8	4	453.9	10.0
5	5	1.4	4	458.3	10.2
6	6	1.1	3	440.6	10.3
7	7	1.0	3	457.2	10.7
8	8	0.9	3	463.9	11.0
9	9	0.0	3	462.3	11.2
10	10	2.4	2	448.2	11.2

Table 1. Ten parameter sets for saccades shown in the simulation section. *PV* and *Amp* denote the peak velocity and amplitude of saccades in normal conditions (i.e., intact OPN), respectively. OPN_{off} was adjusted so that the latency of saccades from the onset of drive phase of the input is 20±1 ms. C_1 and θ were set to 12 and 125, respectively. With these values, the peak velocity, amplitude and latency of the saccade caused by LLBN output alone (corresponding to OPN lesion conditions) were 245.3 deg/s, 9.6 (deg) and 20 ms, respectively. Note that the variability in amplitude in normal conditions depends on the time of resumption of OPN activity. However, all the differences in saccadic amplitude are within a reasonable range (see text for details).

affects the peak velocity of saccades. A smaller T_{rd} needs a larger G_{rd} in order to generate saccades with a particular peak velocity.

In our model, the strength of inhibitory connections from the IBN to the contralateral EBN and IBN (see Fig. 1C for the connection) may affect the peak velocity of saccades in the following manner. An OPN offset would cause post-inhibitory rebound depolarization of MLBNs on both sides, because MLBNs on both sides receive the input from the OPN. Therefore, if the rebound depolarization caused by OPN offset is strong enough to exceed the net threshold, determined by the neuron's threshold plus the amount of inhibitory input from the IBN on the opposite side, the MLBNs would fire. This would also be the case for contralateral saccades, resulting in a reduction of saccadic speed. This frequently happens when the post-inhibitory rebound depolarization is too large, and is the mechanism that underlies the saturation seen in Fig. 2B. Perhaps, for saccades of 10 deg, this kind of behavior might be unrealistic. In our model, inhibitory connections from the IBN help reduce this negative effect by suppressing the rebound depolarization in the MLBNs on the opposite side. However, increasing the strength of the coupling also increases the possibility of oscillations after saccades (e.g., dynamic overshoots), because MLBNs are released from the inhibition of opposite IBNs at the end of contralateral saccades, resulting in post-inhibitory rebound depolarization. As a compromise, we prefer to use weaker connections to reduce the occurrence of oscillations; the weights from EBN to IBN, from IBN to IBN and from IBN to EBN were all set to 0.1 in the simulation data reported here.

OPN_{off} and θ modify saccadic latency before and after an OPN lesion, respectively. Note that setting θ to be larger than the magnitude of the prelude component in the input to MLBNs is necessary to prevent drift before saccades. In the results shown in Fig. 2 and in the following simulated lesion studies, we adjusted these values so that

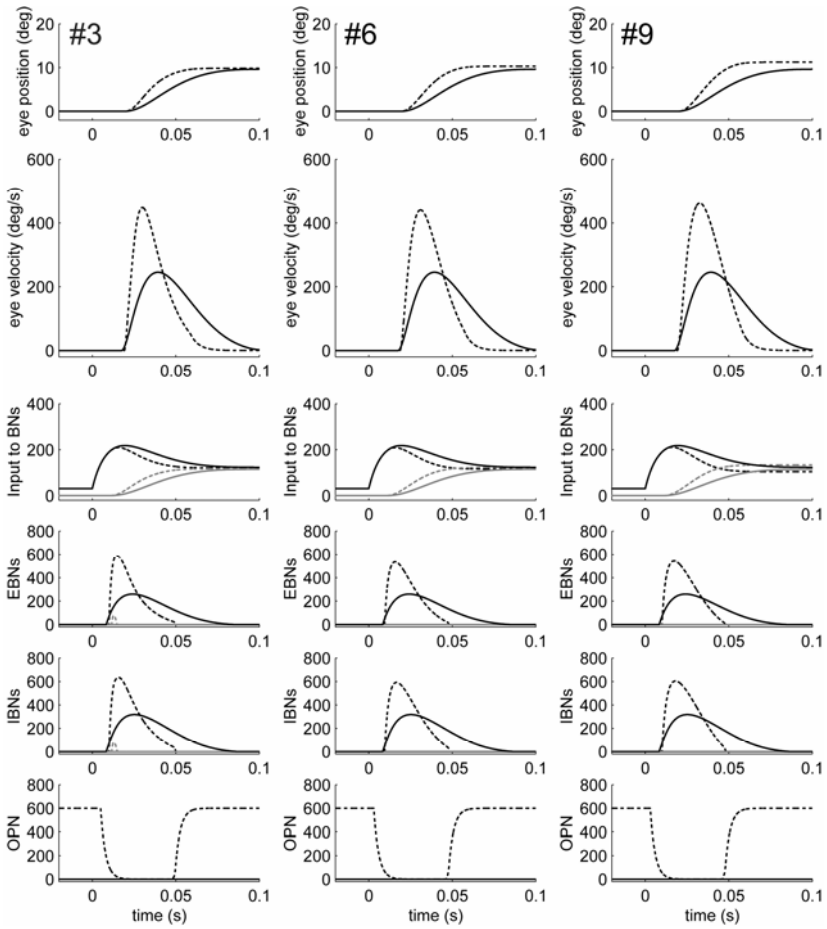

Figure 3. Simulated saccades of 10 deg for three parameter sets (left column for set #3, middle column for set #6 and left column for set #9, see Table 1 for values). From top to bottom rows, temporal traces of eye position, eye velocity and inputs to MLBNs, outputs of EBNs, outputs of IBNs and output of OPN unit are shown. All plots show temporal profiles before (broken line) and after (solid line) an OPN lesion. In the panels for the inputs to MLBNs (EBNs and IBNs), the temporal profiles for the units ipsilateral and contralateral to the saccades are shown in black and gray lines, respectively. (For set #3, contralateral EBNs and IBNs before OPN lesion showed just a tiny blip of activity. For sets #6 and #9, contralateral EBN and IBN before and after OPN lesion showed no response throughout the saccades. It has been reported that some contralateral MLBNs show one or a few spikes near the end of saccades. This property has not been incorporated here, because it does not affect saccade slowing and the general argument in this paper.) Time zero is the beginning of the drive phase of the input to MLBNs.

the lead time of the onset of the drive signal of the LLBN (i.e., the drive phase) was always within 20±1 ms of saccade onset. This simulated the long-lead burst in the input to MLBNs (the actual value of this lead time is unknown, but that is not important here, because it generally does not affect the qualitative properties of saccade slowing after OPN lesion).

3.2 THE EFFECTS OF A SIMULATED OPN LESION

The parameters in the model (C_1, G_{rd}, $\theta$and OPN_{off}) were adjusted by hand so that the model exhibited 10 deg saccades similar to those recorded by Soetedjo et al. [29].

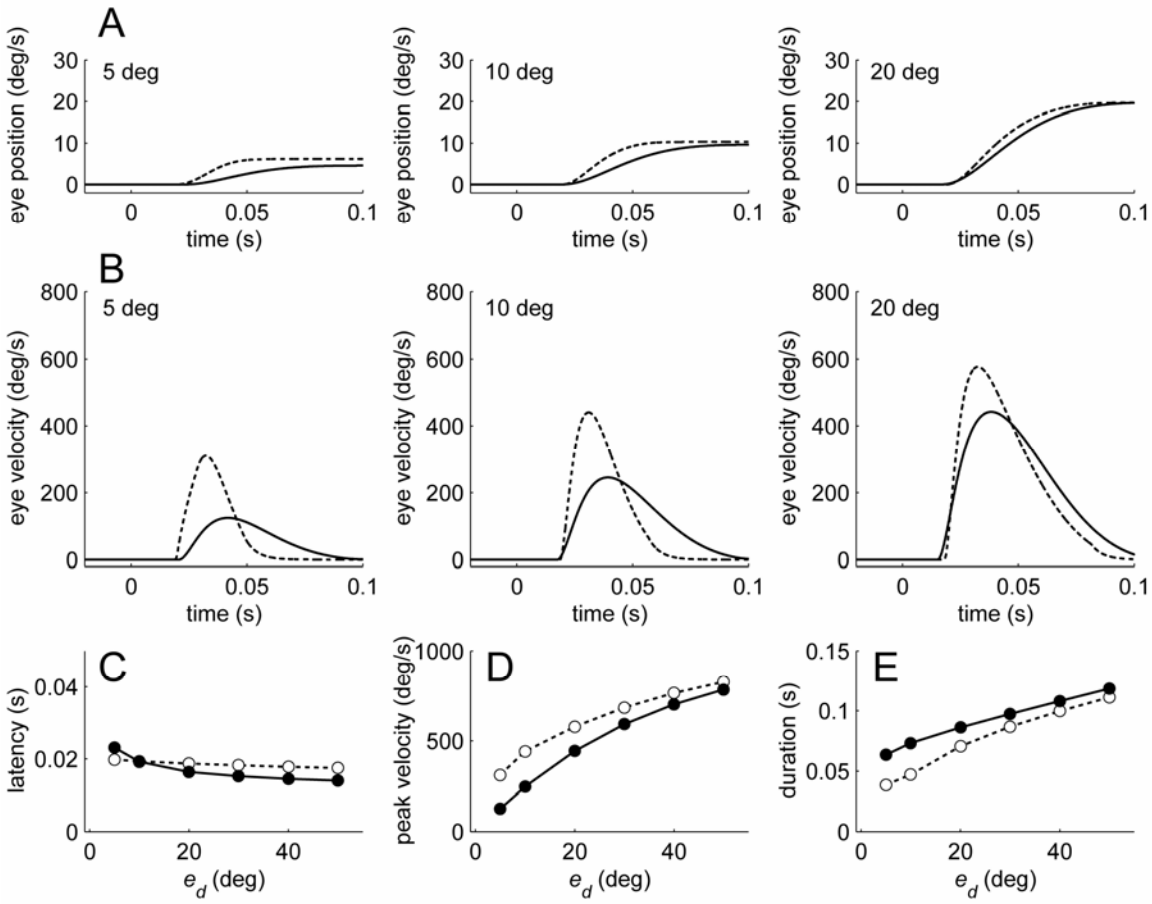

Figure 4. Simulated saccades of different sizes before and after OPN lesion (parameter set #6). **A** and **B** indicate temporal profiles of eye position and velocity of simulated saccades, respectively (left column for saccades of 5 deg, middle for 10 deg and right for 20 deg). The conventions are as in Fig. 3. **C**: latency of saccades from the beginning of the drive phase of the LLBN output as a function of desired eye displacement, e_d. **D**: the peak velocity of saccades. **E**: saccade duration. In **C**, **D** and **E**, open symbols (connected with broken lines) and closed symbols (connected with continuous lines) show measures before and after OPN lesion, respectively. Saccadic duration was measured as the interval between the time points at which the eye velocity first exceeds, until it falls below, 10 deg/s.

That is, the peak velocity of saccades was about 450 deg/s when the OPN was normal and 250 deg/s when the OPN was inactivated. C_1 and θ were 12 and 125, respectively, to generate the expected saccades under OPN lesion conditions (peak velocity of 250 deg/s and latency of 20 ms after the onset of drive phase of the input). Ten sets of parameters that yield the expected saccades described above are listed in Table 1. Examples of 10 deg saccades made before and after an OPN lesion are shown in Fig. 3 for three parameter sets. This figure demonstrates that the saccades produced by the proposed model were robust to the change in parameter sets. As shown in Fig. 3, the saccade slowing after OPN lesion can be produced without a change in reaction time. The duration of saccades generally became longer after an OPN lesion. The amplitude of saccades after the OPN lesion was generally smaller than normal, however the changes were minor. These changes were, in large part, due to the time of resumption of OPN activity. However, their effects were less than 10% of e_d, or less than the speed-related

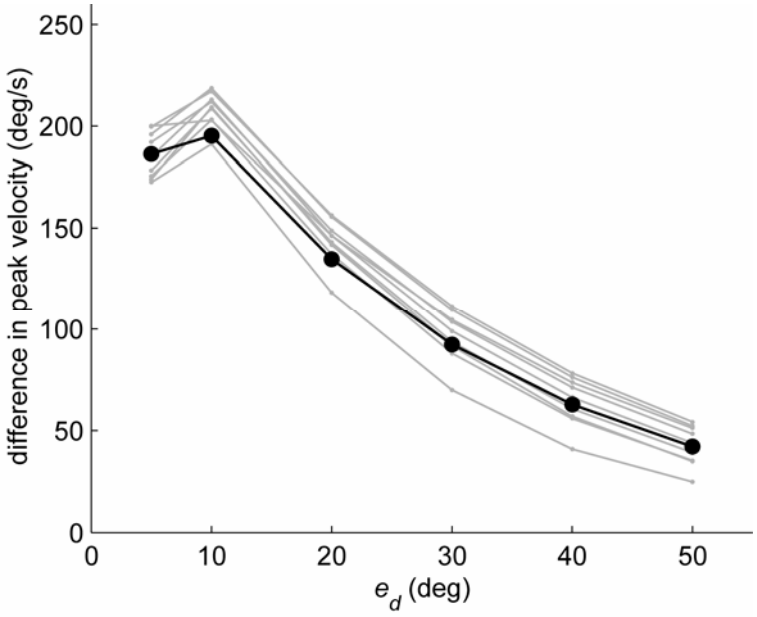

Figure 5. Differences between peak velocities of saccades simulated before and after OPN lesion, as a function of e_d (*before* minus *after*, 10 cases). Circles connected with a black line show the difference in peak velocity of saccades generated by the system with parameter sets #6 (see Table 1 for values), whose temporal profiles of saccades of 10 deg were shown in Fig.4. Gray lines indicate the differences in peak velocity for the nine other sets. This figure represents an easily tested, strong prediction of our model.

change in saccadic amplitude demonstrated by Quaia et al. [41], who showed that a change of 100 deg/s in speed is on average associated with an amplitude change of about 1 deg in nature (see also lesion studies. Table 1). Thus, the model produces behaviors that are consistent with experimental findings from RIP lesions.

Figure 4 shows the dependence on saccade size of the effects of a simulated OPN lesion. Changes in saccadic accuracy after the OPN lesion were minor across saccadic sizes. Although some difference was seen for a saccade of 5 deg (Fig. 4, left column), again all the differences in saccadic amplitude were less than the compensation error above described. Latency of saccades could become longer for smaller saccades or shorter for larger saccades after OPN lesion (Fig. 4C). The amount of change was small across the range of sizes (less than 4 ms for saccades in this example). Such small changes may be difficult to detect in actual data because the variance of saccadic reaction time is generally very large. However, as shown in Fig. 4D and E, the relationship between saccadic size and changes in peak velocity and saccadic duration associated with an OPN lesion show a trend that would be large enough to find in experimental data. That is, the change in peak velocity (and in saccadic duration) was larger for smaller saccadic size. In this example, the decrease of peak velocity of about 60 % was produced for saccades of 5 deg, while less than a 1% decrease occurred for saccades of 50 deg.

Figure 5 shows the differences in peak velocity as a function of saccade size. We show here the property of saccadic peak velocity because it is easily compared to experimental data. As shown in this figure, the curves generally exhibit larger changes in peak velocity for smaller saccades after an OPN lesion. In these cases, changes in peak

velocity for 5 deg saccades were smaller than those for 10 deg saccades. This occurred because of incomplete suppression of an earlier phase of activity in contralateral MLBNs that was more evident for smaller saccadic size, in particular for 5 deg. The mechanism of this behavior of our model has been described earlier in the previous subsection (see above) may be an artifact. However, the monotonic (exponential) decreasing property seen in the larger range of saccadic size (≥ 10deg) derives from the critical hypothesized properties of our MLBN model. In our model, the maintained activity of the OPN is assumed to be independent of the size of the upcoming saccade. As a consequence, the rebound depolarization caused by OPN offset is also independent of saccadic size (i.e., constant). This rebound depolarization is added to the input of MLBNs which is assumed to increase monotonically as saccadic size becomes larger (see definition above). Thus, the proportion of the output of MLBNs due to the rebound depolarization becomes smaller for larger saccade (this shrinkage saturates because of the output nonlinearity of the MLBNs). We propose that this size dependence can be used to test whether our hypothetical mechanism is predominantly responsible for saccade slowing after OPN lesions.

4. DISCUSSION

In the previous section, we showed that the lesion of OPNs in the proposed model elicits behaviors that are consistent with the findings demonstrated by Kaneko [28] and by Soetedjo et al. [29]. In the present scheme, the decrease in peak velocity after OPN lesion is interpreted as the absence of additional drive from post-inhibitory rebound, which would occur in response to OPN offset under normal conditions. As stated previously, this mechanism is independent of any changes in reaction time. That is, no specific changes in reaction time are required to generate the saccade slowing after the OPN lesion. This important property had no explanation before our hypothetical mechanism. The threshold we introduced into MLBN properties allowed the simulation of saccades with very minor differences in reaction time irrespective of OPN conditions, which is also consistent with the experimental finding of no detectable changes in reaction time in most cases. Moreover, maintained accuracy and extended duration were also reproduced because of feedback control of saccades. Thus, all the major behavioral findings from RIP lesion studies have been reproduced by our simulation system with a new MLBN model that has two membrane properties: *post-inhibitory rebound depolarization* and a *threshold for firing*.

4.1 SCOPE OF THE PROPOSED MODEL

This study makes a new theoretical contribution to understanding saccadic control. Here, we have proposed a hypothetical effect of the offset of OPNs on the MLBN contribution to the saccadic drive. The present implementation of the proposed model was done with lumped elements to reduce the complexity of the model structure but to be sufficient to explain the behavioral findings from OPN lesion/inactivation studies. Thus, each element in the proposed model should be considered a computational element rather than a single neuron. Therefore, a single parameter in the proposed model does not reflect a single physiological process, such as a passive membrane time constant, or the opening and closing dynamics of a specific channel, etc., but reflects multiple physiological processes of a population of neurons. In the present study, we

have determined model parameters mainly under behavioral constraints so that the model produces reasonable saccades that are also compatible with the findings from OPN lesion/inactivation studies. Note that we chose them with some consideration of physiological realism, but their values are not known for premotor neurons. Thus, the current scope of the proposed model is at a behavioral level, i.e., eye movements, and shows computational features of the saccade control mechanism, rather than biophysical mechanisms.

Soetedjo et al. [29] also showed two classes of saccade related burst neurons (SRBNs) in superior colliculus. About half of SRBNs exhibited no change in peak activity, but showed extended duration (i.e. slower decay rate) after OPN inactivation. The other half of the SRBNs showed both a decreased peak activity and extended duration after OPN inactivation. The difference in these two populations of SRBNs is outside the scope of this model, because it does not include SRBNs explicitly. In the future, we plan to extend this model to include both classes of SRBNs.

4.2 COMPARISONS WITH OTHER MODELS

Classical models for saccade generation with a negative feedback control scheme that includes a non-linear element [10, 18-20] explained essential properties of normal saccades, e.g. accuracy and non-linear relationship between amplitude and peak-velocity of saccades. Although none of the classical models are able to produce saccade slowing after OPN lesion without changes in latency, the minor change in saccade accuracy (constancy of saccade amplitude) after OPN lesion in our model relies on the negative feedback loop that is common to all classical models since Robinson (1975). The extended duration after OPN lesions also follows naturally as a property of the negative feedback loop.

Scudder's saccade control model differs in several ways from the Robinson model, but still has a local feedback loop [21]. The main feature of the Scudder model is that it uses the LLBNs in the feedforward path. Thus, Scudder's model can produce three of the major findings from OPN lesion studies, i.e. no change in amplitude, extended duration, and slower saccades after OPN lesion. In his model, the LLBN input is the sum of a gaussian pulse (excitatory input from upstream regions, such as the superior colliculus),whose integral over time is set to the desired eye displacement, and an inhibitory burst signal given by inhibitory interneurons from the EBNs (an approximation of eye velocity). Thus, loosely speaking, Scudder's LLBN acts as a comparator between the desired eye displacement and the actual eye displacement, hence providing a drive signal to MLBNs that is related to the motor error. However, it is not equal to motor error, because the LLBNs are an integrator, which spreads the comparison out over time. For normal saccades, the excitatory input signal charges up the LLBN integrator until the OPN unit ceases. This allows the saccade to start and causes an inhibitory signal from the MLBNs to be fed back to the LLBNs. Thus, when OPNs are intact, the MLBNs start their burst with the charged input from LLBNs. When OPNs are inactivated, the input to the LLBNs goes straight through to the MLBNs, and the saccade starts. This makes the initial input to the MLBNs at the start of the saccade very small, because there is no build up on the LLBNs. Thus, the saccade starts too early, and has a lower peak velocity than it would have had if the OPNs had delayed the saccade and allowed the LLBNs to build up more activity. Thus, Scudder's model predicts that the slower saccades after OPN lesions

are a consequence of the earlier triggering of the saccades. However, this early triggering is not consistent with the experimental findings from OPN lesion/inactivation studies, which consistently found no systematic change in saccadic reaction time.

Furthermore, Scudder's model would predict that saccades of all sizes would be slow, because they would all start before the LLBNs could charge up. In contrast, our model clearly indicates that large saccades would be slowed less, because the missing contribution of post-inhibitory rebound is constant (Fig. 5). Thus, a simple experimental test would easily differentiate between these two models.

Enderle [42, 43] proposed a novel model of MLBNs, based on the classic Hodgkin-Huxley membrane equations, wherein the MLBNs are spontaneously active. Thus, this model does not require any drive signals from upstream. Instead, the spontaneous activity of MLBNs is inhibited by OPNs before saccades and resumes after the OPNs cease firing. Enderle also introduced a post-inhibitory rebound property for the MLBNs, by changing effective time constants of sodium and potassium channels (a time-dependent operation that is part of the classical Hodgkin-Huxley equations). As a consequence, after release from inhibition by OPNs an initial bump in the firing rate was seen. Unfortunately, the relationship between an offset of inhibitory input and the modified time constant of these channels was not discussed in his papers. Moreover, the MLBNs were not incorporated into a complete system for generating saccades. Thus, the saccadic behaviors produced by Enderle's model before and after OPN lesion/inactivation have not been defined. In particular, how this MLBN would affect the degree of slowing for different saccade sizes is not clear.

4.3 POSSIBLE TESTS FOR THE PRESENT HYPOTHESIS

The hypothetical mechanism for saccade slowing suggested here relies critically on the existence of post-inhibitory rebound depolarization in MLBNs (especially in EBNs). So far, no study has examined the biophysical properties of MLBNs. Thus, there is currently no evidence for the existence of the neuronal properties we hypothesize here, although both of the properties are common in neurons. The post-inhibitory rebound depolarization has been examined in neurons in deep cerebellar nuclei [44] and in the medial vestibular nucleus in the brainstem [45]. Examining properties of monkey MLBNs with similar methods to those in the previous studies would test the minimum requirements of our hypothesis, i.e. the existence of the hypothetical membrane properties. Moreover, this experiment may provide quantitative details of post-inhibitory rebound depolarization that would help to improve the model used here.

In the Results section, we adjusted the parameters so that the model generated saccade slowing that was comparable to the examples demonstrated by Soetedjo et al. [29]. As described above, a decrease of about 60% was achieved for the saccade of 5 deg in the example shown in Fig. 4. This amount is between the largest and the second largest decrease reported in Soetedjo et al. [29]. In the parameter sets in Table 1, the decreases for saccades of 5 deg ranged from 58-62%. In fact, the model generated a difference of about 70% for 5 deg saccades after an OPN lesion with the use of a smaller C_1, which determines the peak velocity in the OPN lesion condition (not shown). The decrease by 70% is the maximum reported after muscimol injections into RIP in a monkey. Thus, the proposed mechanism can produce huge decreases in peak velocity after an OPN lesion, just as was observed in experimental studies.

However, it is still in question whether our hypothetical mechanism is fully responsible for such large changes in peak velocity after an OPN lesion. It is well known that the relationship between duration and size is almost linear in the range from 5 deg to 30 deg in normal subjects [46-48]. While here, with the parameters we have shown in the previous section, relationships between saccadic duration and size were frequently curved (although the magnitude of deviations from the linear property was quite sensitive to the method used to estimate saccadic duration from our simulation data). Figure 4E shows that the relationship between the saccadic size and duration was not linear for saccades between 10 and 20 deg in the normal case, whereas it was very linear after an OPN lesion. A possible reason for this violation is that the increase in saccadic speeds for smaller saccades caused by the post-inhibitory rebound depolarization is too large relative to those for larger saccades. However, it is also possible that the implementation of the saccadic system used here to control the dynamics at the end of saccades, which greatly affect the measurements of saccadic duration, is insufficient to reproduce this relationship exactly.

Examining the characteristic change in peak velocity after OPN lesion, as shown in Fig. 5, i.e., smaller changes in peak velocity for larger saccades, would be an easy test of whether our hypothesis alone is responsible for saccade slowing after an OPN lesion. As stated in the previous section, this characteristic is due to the decreased efficacy of the post-inhibitory rebound, produced independently from saccadic size by the saturation nonlinearity in our MLBN model, and hence is an inherent property of our hypothetical mechanism. Note that this characteristic can be easily tested using a simple experimental technique, i.e., a visually guided saccade paradigm with a muscimol injection into the RIP, which has already been developed by Kaneko and colleagues.

Our model predicts that the blockade of IPSP channels on ipsilateral EBNs would exhibit similar effects to an OPN lesion on saccades (not shown). This is because both perturbations remove the additional drive of post-inhibitory rebound depolarization induced by OPN offset that would occur in normal conditions. This prediction is testable because this blockade can be achieved with a conventional, chemical injection technique. Fortunately, the neurotransmitter of OPNs is known to be glycine [49]. Therefore, the injection of strychnine, an antagonist of glycine receptors, would be the most reasonable choice to test our hypothesis. Of importance to this proposed experiment is that this tests any contribution of the hypothetical mechanism proposed here to the saccade slowing after an OPN lesion. If our hypothetical mechanism contributes, at least in part, to slowing down the saccades, a decrease in peak velocity will be observed after blocking the inhibitory synaptic receptors of EBNs mediating the hyperpolarizing input from OPNs, i.e., glycine receptors. Lesion of the RIP region may consist of effects other than silencing the OPNs (although this is currently unknown). Therefore, results from this proposed experiment would tell us whether our hypothetical mechanism is fully, or only partially, responsible for saccade slowing.

In this study, we hypothesized that the threshold in MLBN membrane properties may compensate for the loss of the classical function of OPNs, i.e., the inhibitory gate. However, it is still possible that there may be a second class of pause neurons that behaves like OPNs and lies in a different region from that of OPNs (we did not implement this possibility in this study), although no report has been made of such neurons. If there are no other neurons that duplicate OPN functions, and if there are no

threshold in MLBNs, eye drift before saccades in response to the prelude component of the input has to be observed after complete blocking of inhibitory receptors on EBNs. If the current hypothesis is correct, such a “prelude” eye movement does not occur even after completely blocking the inhibitory synaptic receptors, because of the threshold mechanism. Thus, blocking inhibitory receptors on EBNs may also help test this threshold hypothesis.

In previous models of saccade control [10, 18-26], the MLBNs are described as simple elements that have at most a single time constant, a firing rate saturation, and a delay. Hence, they have no influence on saccade dynamics. The hypothetical mechanism for saccade slowing proposed in the present study suggests possible functional roles for MLBNs and OPNs in determining saccadic dynamics, in this case speed and latency. However, the hypothetical mechanism is based on the membrane properties of MLBNs whose characteristics, or even existence, have yet to be discovered. Results from the experiments proposed above would test the feasibility of our hypothesis and would offer useful suggestions for improving the hypothesis and/or its implementation, leading to a better understanding of the premotor structures of saccade generation.

REFERENCES

[1] K. Hepp, V. Henn, T. Vilis, and B. Cohen, "Brainstem regions related to saccade generation," in *The Neurobiology of Saccadic Eye Movements, Reviews of Oculomotor Research, Vol. III*, R. H. Wurtz and M. E. Goldberg, Eds. Amsterdam: Elsevier, 1989, pp. 105-212.

[2] C. A. Scudder, C. S. Kaneko, and A. F. Fuchs, "The brainstem burst generator for saccadic eye movements: a modern synthesis," *Exp. Brain. Res.*, vol. 142, pp. 439-62, 2002.

[3] D. L. Sparks, "The brainstem control of saccadic eye movements," *Nat Rev Neurosci*, vol. 3, pp. 952-64, 2002.

[4] O. Hikosaka, Y. Igusa, and H. Imai, "Inhibitory connections of nystagmus-related reticular burst neurons with neurons in the abducens, prepositus hypoglossi and vestibular nuclei in the cat," *Exp Brain Res*, vol. 39, pp. 301-11, 1980.

[5] J. A. Büttner-Ennever and U. Büttner, "The reticular formation," in *Neuroanatomy of the Oculomotor System*, J. A. Büttner-Ennever, Ed. Amsterdam: Elsevier, 1988, pp. 119-176.

[6] A. Strassman, S. M. Highstein, and R. A. McCrea, "Anatomy and physiology of saccadic burst neurons in the alert squirrel monkey. II. Inhibitory burst neurons," *J. Comp. Neurol.*, vol. 249, pp. 358-80, 1986.

[7] A. Strassman, S. M. Highstein, and R. A. McCrea, "Anatomy and physiology of saccadic burst neurons in the alert squirrel monkey. I. Excitatory burst neurons," *J. Comp. Neurol.*, vol. 249, pp. 337-57, 1986.

[8] C. A. Scudder, A. F. Fuchs, and T. P. Langer, "Characteristics and functional identification of saccadic inhibitory burst neurons in the alert monkey," *J. Neurophysiol.*, vol. 59, pp. 1430-1454, 1988.

[9] E. L. Keller, "Participation of medial pontine reticular formation in eye movement generation in monkey," *J Neurophysiol*, vol. 37, pp. 316-32., 1974.

[10] J. A. Van Gisbergen, D. A. Robinson, and S. Gielen, "A quantitative analysis of generation of saccadic eye movements by burst neurons," *J Neurophysiol*, vol. 45, pp. 417-42., 1981.

[11] B. Cohen and V. Henn, "Unit activity in the pontine reticular formation associated with eye movements," *Brain Res.*, vol. 46, pp. 403-410, 1972.

[12] E. S. Luschei and A. F. Fuchs, "Activity of brain stem neurons during eye movements of alert monkeys," *J. Neurophysiol.*, vol. 35, pp. 445-461, 1972.

[13] J. A. Buttner-Ennever, B. Cohen, M. Pause, and W. Fries, "Raphe nucleus of the pons containing omnipause neurons of the oculomotor system in the monkey, and its homologue in man," *J Comp Neurol*, vol. 267, pp. 307-21, 1988.

[14] K. Yoshida, Y. Iwamoto, S. Chimoto, and H. Shimazu, "Saccade-related inhibitory input to pontine omnipause neurons: an intracellular study in alert cats," *J Neurophysiol*, vol. 82, pp. 1198-208, 1999.

[15] A. Strassman, C. Evinger, R. A. McCrea, R. G. Baker, and S. M. Highstein, "Anatomy and physiology of intracellularly labelled omnipause neurons in the cat and squirrel monkey," *Exp Brain Res*, vol. 67, pp. 436-40, 1987.

[16] T. P. Langer and C. R. Kaneko, "Brainstem afferents to the oculomotor omnipause neurons in monkey," *J. Comp. Neurol.*, vol. 295, pp. 413-27, 1990.

[17] E. L. Keller and J. A. Edelman, "Use of interrupted saccade paradigm to study spatial and temporal dynamics of saccadic burst cells in superior colliculus in monkey," *J Neurophysiol*, vol. 72, pp. 2754-70., 1994.

[18] D. A. Robinson, "Oculomotor control signals," in *Basic Mechanisms of Ocular Motility and Their Clinical Implications*, G. Lennerstrand and P. Bach-y-Rita, Eds. Oxford: Pergamon Press, 1975, pp. 337-374.

[19] D. S. Zee and D. A. Robinson, "A hypothetical explanation of saccadic oscillations," *Ann. Neurol.*, vol. 5, pp. 405-414, 1979.

[20] R. Jürgens, W. Becker, and H. H. Kornhuber, "Natural and drug-induced variations of velocity and duration of human saccadic eye movements: Evidence for a control of the neural pulse generator by local feedback," *Biol. Cybern.*, vol. 39, pp. 87-96, 1981.

[21] C. A. Scudder, "A new local feedback model of the saccadic burst generator," *J. Neurophysiol.*, vol. 59, pp. 1455-1475, 1988.

[22] P. Dean, "Modelling the role of the cerebellar fastigial nuclei in producing accurate saccades: the importance of burst timing.," *Neurosci.*, vol. 68, pp. 1059-1077, 1995.

[23] C. Quaia and L. M. Optican, "Model with distributed vectorial premotor bursters accounts for the component stretching of oblique saccades," *J. Neurophysiol.*, vol. 78, pp. 1120-1134, 1997.

[24] P. Lefèvre, C. Quaia, and L. M. Optican, "Distributed model of control of sacades by superior colliculus and cerebellum," *Neural Networks*, vol. 11, pp. 1175-1190, 1998.

[25] K. Arai, S. Das, E. L. Keller, and E. Aiyoshi, "A distributed model of the saccade system: simulations of temporally perturbed saccades using position and velocity feedback," *Neural Networks*, vol. 12, pp. 1359-1375, 1999.

[26] L. M. Optican and Q. Quaia, "From sensory space to motor commands: Lessons from saccades," *Proc IEEE EMBC Conf*, vol. 1, pp. 820-23, 2001.

[27] C. Quaia, P. Lefèvre, and L. M. Optican, "Model of the control of saccades by superior colliculus and cerebellum," *J. Neurophysiol.*, vol. 82, pp. 999-1018., 1999.

[28] C. R. Kaneko, "Effect of ibotenic acid lesions of the omnipause neurons on saccadic eye movements in rhesus macaques," *J. Neurophysiol.*, vol. 75, pp. 2229-42, 1996.

[29] R. Soetedjo, C. R. Kaneko, and A. F. Fuchs, "Evidence that the superior colliculus participates in the feedback control of saccadic eye movements," *J. Neurophysiol.*, vol. 87, pp. 679-95, 2002.

[30] D. S. Zee, L. M. Optican, J. D. Cook, D. A. Robinson, and W. K. Engel, "Slow saccades in spinocerebellar degeneration," *Arch. Neurol.*, vol. 33, pp. 243-251, 1976.

[31] C. R. Kaneko, "Hypothetical explanation of selective saccadic palsy caused by pontine lesion," *Neurology*, vol. 39, pp. 994-5, 1989.

[32] S. Ramat, R. J. Leigh, D. S. Zee, and L. M. Optican, "Coupling and post-inhibitory rebound firing in brain stem excitatory and inhibitory burst neruons may explain high-frequency saccadic oscillations," *Soc. Neurosci. Abstr.*, pp. #716.7, 2002.

[33] K. Miura and L. M. Optican, "Saccadic slowing after inactivation of omnipause neuron may be caused by the membrane characteristics of brain stemburst neurons," *Soc. Neurosci. Abstr.*, pp. #716.8, 2002.

[34] K. Miura and L. M. Optican, "Membrane properties of medium-lead burst neurons may contribute to dynamical properties of saccades," *Proceedings of the 1st International IEEE EMBS Conference on Neural Engineering*, pp. In Press, 2003.

[35] S. Chimoto, Y. Iwamoto, H. Shimazu, and K. Yoshida, "Monosynaptic activation of medium-lead burst neurons from the superior colliculus in the alert cat," *J Neurophysiol*, vol. 75, pp. 2658-61, 1996.

[36] E. L. Keller, R. M. McPeek, and T. Salz, "Evidence against direct connections to PPRF EBNs from SC in the monkey," *J Neurophysiol*, vol. 84, pp. 1303-13, 2000.

[37] D. L. Sparks, "Functional properties of neurons in the monkey superior colliculus: coupling of neuronal activity and saccade onset," *Brain Res*, vol. 156, pp. 1-16, 1978.

[38] C. A. Scudder, A. K. Moschovakis, A. B. Karabelas, and S. M. Highstein, "Anatomy and physiology of saccadic long-lead burst neurons recorded in the alert squirrel monkey. II. Pontine neurons," *J Neurophysiol*, vol. 76, pp. 353-70, 1996.

[39] H. Noda, S. Sugita, and Y. Ikeda, "Afferent and efferent connections of the oculomotor region of the fastigial nucleus in the macaque monkey," *J Comp Neurol*, vol. 302, pp. 330-48, 1990.

[40] K. Ohtsuka and H. Noda, "Saccadic burst neurons in the oculomotor region of the fastigial nucleus of macaque monkeys," *J Neurophysiol*, vol. 65, pp. 1422-34, 1991.

[41] C. Quaia, M. Pare, R. H. Wurtz, and L. M. Optican, "Extent of compensation for variations in monkey saccadic eye movements," *Exp Brain Res*, vol. 132, pp. 39-51., 2000.

[42] J. D. Enderle and E. J. Engelken, "Simulation of oculomotor post-inhibitory rebound burst firing using a Hodgkin-Huxley model of a neuron," *Biomed Sci Instrum*, vol. 31, pp. 53-8, 1995.

[43] J. D. Enderle, "Neural control of saccades," *Prog Brain Res*, vol. 140, pp. 21-49, 2002.

[44] C. D. Aizenman and D. J. Linden, "Regulation of the rebound depolarization and spontaneous firing patterns of deep nuclear neurons in slices of rat cerebellum," *J. Neurophysiol.*, vol. 82, pp. 1697-709, 1999.

[45] C. Sekirnjak and S. du Lac, "Intrinsic firing dynamics of vestibular nucleus neurons," *J. Neurosci.*, vol. 22, pp. 2083-95, 2002.

[46] A. F. Fuchs, "The saccadic system," in *The Control of Eye Movements*, P. Bach-y-Rita, C. C. Collins, and J. E. Hyde, Eds. NY and London: Academic Press, 1971, pp. 343-362.

[47] W. Becker, "Metrics," in *The Neurobiology of Saccadic Eye Movements, Reviews of Oculomotor Research, Vol. III*, R. H. Wurtz and M. E. Goldberg, Eds. Amsterdam: Elsevier, 1989.

[48] R. J. Leigh and D. S. Zee, *The Neurology of Eye Movements*, Third ed. New York: Oxford, 1999.

[49] A. K. Horn, J. A. Buttner-Ennever, P. Wahle, and I. Reichenberger, "Neurotransmitter profile of saccadic omnipause neurons in nucleus raphe interpositus," *J Neurosci*, vol. 14, pp. 2032-46, 1994.